HHS Public Access

Author manuscript

ACS Appl Mater Interfaces. Author manuscript; available in PMC 2021 March 29.

Published in final edited form as:

ACS Appl Mater Interfaces. 2017 May 10; 9(18): 15254–15264. doi:10.1021/acsami.7b01408.

Tunable Nitric Oxide Release from *S*-nitroso-*N*-acetylpenicillamine via Catalytic Copper Nanoparticles for Biomedical Applications

Jitendra Pant[a], **Marcus J. Goudie**[a], **Sean Hopkins**[a], **Elizabeth J. Brisbois**[b], **Hitesh Handa**[a,*]

[a]School of Chemical, Materials and Biomedical Engineering, University of Georgia, Athens, USA

[b]Department of Surgery, University of Michigan, Ann Arbor, USA

Abstract

The quest for novel therapies to prevent bacterial infections and blood clots (thrombosis) is of utmost importance in biomedical research due to exponential growth in cases of thrombosis, blood infections, and the emergence of multi-drug resistant strains of bacteria. Endogenous nitric oxide (NO) is a cellular signaling molecule that plays a pivotal role in host immunity against pathogens, prevention of clotting, and regulation of systemic blood pressure among several biological functions. The physiological effect of NO is dose dependent that necessitates the need of tunable release kinetics which is the objective of this study. In the present study, polymer composites were fabricated by incorporating *S*-nitroso-*N*-acetylpenicillamine (SNAP) in a medical grade polymer, Carbosil, and top coated with varying levels of catalytic copper nanoparticles (Cu-NPs). The addition of Cu-NPs increased the NO release as well as the overall antimicrobial activity via its oligodynamic effect. The 10 wt% SNAP composites (without Cu-NPs coats) showed an NO flux of $1.32 \pm 0.6 \times 10^{-10}$ mol min^{-1} cm^{-2}, while Cu-NPs incorporated SNAP films exhibited a flux of $4.48 \pm 0.5 \times 10^{-10}$, $4.84 \pm 0.3 \times 10^{-10}$, and $11.7 \pm 3.6 \times 10^{-10}$ mol min^{-1} cm^{-2} with 1 wt%, 3 wt%, and 5 wt% Cu-NPs respectively. This resulted in a significant reduction (up to 99.8%) in both gram-positive and gram-negative bacteria with very low platelet adhesion (up to 92% lower) as compared to the corresponding controls. Copper leachates from the SNAP films were detected using ICP-MS technique and were found to be significantly lower than the recommended safety limit by the FDA. The cell viability test performed on mouse fibroblast 3T3 cells provides a supportive evidence for the biocompatibility of the material *in vitro*.

Graphical Abstract

*Corresponding author: Hitesh Handa, School of Chemical, Materials, and Biomedical Engineering, University of Georgia, 220 Riverbend Road, Athens, GA 30605, Telephone: (706) 542-8109, hhanda@uga.edu.

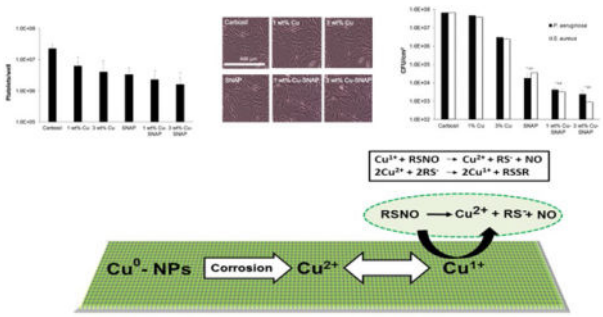

Keywords

nitric oxide; *S*-nitroso-*N*-acetylpenicillamine; copper nanoparticles; infections; cytotoxicity; controlled release

1. Introduction

With over 8000 medical devices entering the market every year, the United States has the biggest medical device market in the world with an estimated market size of approximately $133 billion in 2016.[1] Unfortunately, infection and blood clotting (thrombosis) remain the major risks associated with the application of medical devices in humans. There is an exponential increase in nosocomial infections due to the rapid development of multi-drug resistant strains and failure of the current antimicrobial strategies to prevent this. Similarly, blood clotting on the implants' surface is a complex medical problem, as they can break loose, and cause pulmonary embolism (blocked blood flow in lungs) by traveling to the lungs through the blood stream. These two issues not only put the patient's life at risk but also delay their health recovery ultimately adding to the healthcare costs. The failure of currently available antimicrobials and antithrombotic agents to control these problems has spurred the development of new biocompatible and hemocompatible materials.

In the US alone there are over 1.7 million Hospital Acquired Infections (HAIs) cases annually resulting in 100,000 deaths.[1–3] Biofilm accumulation not only resists the action of bactericidal agents but can ultimately degrade the polymeric material used in device fabrication.[4–5] This can potentially lead to serious consequences like the release of toxic degradation products, bacteremia, and septicemia. The current state-of-the-art mainly uses antimicrobial agents like antibiotics or silver nanoparticles (Ag-NPs) with commercialized biomedical implants. Several studies have found Ag-NPs to be cytotoxic to human dermal fibroblast,[6] mice peritoneal macrophage cell products,[7] rat hepatocytes,[8] and both genotoxic and cytotoxic to human lung fibroblast cells.[9] These findings are in line with the cell membrane disruption and oxidative stress caused by Ag-NPs when tested on mouse fibroblast cells.[10] Similarly, the use of antibiotics has been a concern for the past few decade due to emerging issues of antibiotic resistance in bacteria.[11–12] Another important determinant for increasing chances of clinical success of a biomedical implant in the blood is the suppression of platelet activation which ultimately prevent thrombosis.[13–14] Even though heparin is a widely used and popular thrombotic agent to prevent blood clots, it can

lead to side effects such as increased risk of hemorrhage and thrombocytopenia in addition to not being effective in 33% of the intensive unit care patients.[15–16]

Recommendations from the studies suggest that there is a need to develop new biomaterials that should not only be able to inhibit drug-resistant bacteria but should also be hemocompatible without causing the undesirable side effects such as cytotoxicity. In the last few decades, nitric oxide (NO) based therapies have emerged as a potential bactericide and antithrombotic alternatives to the current state of the art to prevent pathogenic infections and clot formation in the medical implants. Nitric oxide is a cellular signaling molecule in animals including humans with a very short half-life (<5 sec) that plays a pivotal role immunity, prevention of clots, regulation of systemic blood pressure, vascular remodeling and angiogenesis regulating other biological functions such as inflammation and cell proliferation.[17–19] Healthy endothelial cells exhibit an estimated NO flux of $0.5–4.0 \times 10^{-10}$ mol cm^{-2} min^{-1} to maintain vascular tone.[20] The NO released within the sinus cavities and macrophages functions as a natural antimicrobial agent to combat pathogen invasion in humans.[21–23]

Multiple studies have reported the antibacterial and antithrombic success of NO obtained from various NO donors. The antibacterial effect of NO has been proven against infection causing agent pathogens such as *Staphylococcus aureus*,[24–25] *Staphylococcus epidermis*,[24] *Pseudomonas aeruginosa*,[26–27] *Escherichia coli*,[24–25, 28] *Acinetobacter baumanii*,[29–30] *Listeria monocytogenes*, and *Enterococcus faecalis*.[31] The antimicrobial mechanisms of NO include nitrosation of amines and thiols in the extracellular matrix, lipid peroxidation and tyrosine nitration in the cell wall, and DNA cleavage in the cellular matrix.[32] Moreover, the use of NO is unlikely to stimulate the production of resistant strains due to rapid reduction of microbial load.[26, 33–34] On the other hand, the ability of NO to prevent blood clots in the implants is due to its ability to inhibit platelet activation and adhesion of blood platelet cells on the surface which marks the initial phase of thrombosis.[18]

The potential role of endogenously released NO in controlling physiological processes has also led to the development of NO-releasing/generating materials which can provide an exogenous supply of NO to be utilized in biomedical applications.[14, 35–36] In general, the current NO releasing strategies can be achieved by two mechanisms: (i) NO generating materials (NOgen) that alters the endogenous NO production from the physiological NO donors such as nitrosothiols (RSNOs) using catalytic metal ions, heat, light or temperature as stimulants; and (ii) NO releasing (NOrel) exogenous NO donor molecules that actively release NO or its redox analogs.[37] The NOgen materials include several high and low molecular weight RSNOs including *S*-nitroso-albumin (high molecular weight), *S*-nitroso-cysteine, and *S*-nitroso-glutathione (both low molecular weight). The catalytic generation of NO from naturally occurring RSNOs has resulted in a number of NOgen materials, where material structures such as metal organic frameworks or zeolites have been used to provide copper catalyzed generation of NO for both organic NO donors (such as nitrates and nitrites) as well as RSNOs.[36, 38–39]

Incorporation of external RSNOs within hydrophobic polymers has been shown to provide physiological NO release rates from the polymeric surface, reducing thrombus formation

and bacterial adhesion both *in vitro* and *in vivo*.[40] Multiple studies have shown the use of NO donor systems like *S*-nitroso-*N*-acetylpenicillamine (SNAP), *N*-diazeniumdiolated dibutyl hexane diamine (DBHD/N_2O_2), *S*-nitroso-*N*-acetylcysteine (SNAC), and NO releasing metal organic framework.[13–14, 40–41] Out of these NO donors, SNAP has been used extensively for active NO release for multiple biomedical applications.[31, 42–45] Polymers with SNAP incorporation have been shown to release NO consistently for over 2 weeks but near the lower end of physiological levels.[46] Although very effective, the ability to maintain NO release at a level within the physiological limits (preferably at the upper end) would be beneficial for reproducibility, reliability, and increased efficacy for various biomedical applications. The ultimate effect of NO on pathogens, blood activity as well as mammalian cells is dose dependent, therefore NO release can potentially be regulated via a catalyst/stimulant when using NO donors as therapeutic agents.[47–48] One such mean to increase the release rate, such as the exposure to light, has shown an excellent control of NO release.[49] While these materials may be useful for applications such as extracorporeal circuits, where the device remains outside of the body, these materials may have a limited applicability for implanted medical devices that remain inside the body as applying light to these areas is not feasible. Therefore, developing materials where NO release at the material/tissue interface can be controlled with an incorporated catalyst, such as copper nanoparticles (Cu-NPs), will be highly advantageous for long-term *in vivo* medical applications. From the application point of view, this strategy will not only ensure the long-term active supply of exogenous NO via SNAP at the site of application but will also provide the stimulation for enzymatic NO release via the action of copper ions on endogenous RSNOs in the blood.[39] In addition, copper ions possess oligodynamic effect i.e. they have inherent antibacterial properties which would work synergistically with NO to bring enhance the antibacterial effect.[50]

To summarize, the addition of the Cu-NPs will not only provide a method to catalytically control the level of NO released from the physically blended NO donor but also provides NO generating capabilities by utilizing endogenous NO donors in the blood when used in blood contacting applications besides its oligodynamic effect. In this study, we fabricated a novel composite material with the incorporation of SNAP in a medical grade polymer, Carbosil™. The resulting composite was coated with varying concentrations of the Cu-NPs layer to catalyze the *in-situ* release of NO from the synthetic NO donor SNAP via copper ions. These materials were then examined for NO release kinetics, platelet adhesion, bacterial inhibition, and cytotoxicity besides other physical and chemical characterizations.

2. Materials and Methods

2.1 Materials

N-Acetyl-*D*-penicillamine (NAP), potassium chloride, sodium chloride, potassium phosphate monobasic, sodium phosphate dibasic, tetrahydrofuran (THF), ethylenediaminetetraacetic acid (EDTA), sulfuric acid and *N, N*-dimethylacetamide (DMAc) were purchased from Sigma-Aldrich (St. Louis, MO). Carbosil™ 20 80A (here on will be referred to as Carbosil) was obtained from DSM (Berkeley, CA). LB broth and LB Agar were obtained from Fisher Bioreagents (Fair Lawn, NJ). Phosphate buffered saline (PBS), pH 7.4, containing 138 mM NaCl, 2.7 mM KCl, 10 mM sodium phosphate, was used for all

in vitro experiments. Dulbecco's modification of Eagle's medium (DMEM) and trypsin-EDTA were purchased from Corning (Manassas, VA 20109). The Cell Counting Kit −8 (CCK-8) was obtained from Sigma-Aldrich (St Louis MO 63103). The antibiotic Penicillin-Streptomycin (Pen-Strep) and fetal bovine serum (FBS) were purchased from Gibco-Life Technologies (Grand Island NY 14072). The LDH kit was purchased from Roche Life Sciences (Indianapolis, IN). The Copper nanoparticles (99%, 40–60 nm) were obtained from SkySpring Nanomaterials, Inc. (Houston, TX). The bacterial strains *Pseudomonas aeruginosa* (ATCC 27853) and *Staphylococcus aureus* (ATCC 5538) and mouse 3T3 cells (ATCC 1658) were originally obtained from American Type Culture Collection (ATCC).

2.2.1 Synthesis of SNAP—Synthesis of SNAP was done through a modified version of a previously reported method.[51] Sodium nitrite and NAP were added in an equimolar ratio to a 1:1 mixture of methanol and water containing 2M H_2SO_4 and 2M HCl. The mixture was stirred in dark (to protect from NO release by light stimulation) for 40 min using a magnetic stirrer. Thereafter, the reaction vessel was placed in an ice bath to precipitate the SNAP crystals. The resulting crystals were filtered, rinsed, and dried under vacuum in the dark, and were stored at −20°C before their use in the experiment.

2.2.2 Fabrication of Copper-NPs doped NO generating composites—SNAP composites were prepared by initially dissolving 70 mg of Carbosil-2080A per mL of THF in an amber vial by stirring for 1h at room temperature using a magnetic stirrer. Once completely dissolved, 10 wt% SNAP (7mg/mL) was added and quickly dissolved for 2 min. The resulting solution was cast in Teflon™ molds (diameter = 2.5cm) and dried overnight in the dark to prevent undesired light-induced NO release from the SNAP. To ensure that there were no traces of residual THF, the films were further vacuum dried using a desiccator at room temperature. The control Carbosil films were prepared in a similar manner but excluded the addition of SNAP. The SNAP and Carbosil films were dip-coated twice with Carbosil (50 mg/mL) or the Cu-NPs (1, 3, or 5 wt% Cu-NPs (w/w)) dispersed in 50mg/mL of Carbosil solution. All the films were finally top coated with a layer of Carbosil (50 mg/mL) to prevent leaching of SNAP and/or Cu-NPs from the films. A representative cartoon of Cu-SNAP films is shown in Figure 1. Altogether four different types of polymeric composites and their respective controls (without SNAP) were fabricated:

1. SNAP composite: Carbosil (70 mg/mL) incorporating 10 wt% SNAP along with three top coats of Carbosil (50 mg/mL) to reduce leaching of SNAP
2. 1 wt% Cu-SNAP composite: SNAP composite with two intermediate coats of 1 wt% Cu-NPs and one top coat of (50 mg/mL) Carbosil
3. 3 wt% Cu-SNAP composite: SNAP composite with two intermediate coats of 3 wt% Cu-NPs and one top coat of (50 mg/mL) Carbosil
4. 5 wt% Cu-SNAP composite: SNAP composite with two intermediate coats of 5 wt% Cu-NPs and one top coat of (50 mg/mL) Carbosil

2.2.3 Surface morphology characterization (SEM)—All configurations of the Cu-SNAP composite films were examined under a scanning electron microscope (SEM) (FEI Inspect F FEG-SEM) to study the surface morphology of the polymeric composite. The top

coat solution of 3 wt% Cu-NPs in Carbosil (50 mg/mL) was cast into a film in a Teflon mold (d = 2.5 cm), dried, and examined for roughness using SEM. Dried film samples were mounted on a metal stub with double-sided carbon tape and sputter coated with 10 nm gold-palladium using a Leica EM ACE200 sputter coater. Images were taken at accelerating voltage 5 kV.

2.2.4 NO release kinetics—Nitric oxide released from the polymeric composites was measured using a Sievers Chemiluminescence Nitric Oxide Analyzer (NOA) 280i (Boulder, CO). Polymeric films were placed in the sample vessel immersed in PBS (pH 7.4) and maintained at 37 °C. Buffer for control samples also contained 100 μM EDTA to quench all metal ion activity in the buffer solution. Buffer samples containing films with copper top coats contained no EDTA to allow for the catalytic activity of copper. Nitric oxide was continuously purged from the buffer and swept from the headspace using nitrogen sweep gas and bubbler into the chemiluminescence detection chamber. Films were submerged in PBS in glass vials, and kept at 37 °C between NO release measurements. The fresh buffer was used for each NO release measurement, and films were kept in fresh buffer for storage after each measurement. Nitric oxide release measurements were also conducted after exposure of the films to bacterial suspensions to confirm that NO was continued to be released throughout the entire exposure, as well as demonstrate the presence of bacteria and the medium had an insignificant effect on the release kinetics.

2.2.5 In vitro platelet adhesion—Fresh porcine blood was drawn into a BD 60 mL syringe with 3.4% sodium citrate at a blood: citrate ratio of 9:1 through a blind draw at the Large Animal Research Unit at the University of Georgia School of Animal and Dairy Science, Athens, GA. Immediately following the draw, the anticoagulated blood was centrifuged at 1200 rpm for 12 min using the Eppendorf Centrifuge 5702. The platelet rich plasma (PRP) portion was collected carefully with a pipette as to not disturb the buffy coat. The remaining samples were then spun again at 4000 rpm for 20 min to achieve platelet poor plasma (PPP). Total platelet counts in both the PRP and PPP fractions were determined using a hemocytometer (Fisher). The PRP and PPP were combined in a ratio to give a final platelet concentration ca. 2×10^8 platelets/mL. Calcium chloride ($CaCl_2$) was added to the final platelet solution to achieve a final concentration of 2.5 mM to reverse the effect of the anticoagulant during the experiment.

The degree of platelet adhesion was determined using a Roche lactate dehydrogenase (LDH) Cytotoxicity Detection Kit in a 96-well format as per the supplier's specifications. Each well was coated with the respective combination of control/NO releasing and control/Cu particle solutions. Coating of the wells was done in three stages: 1) a base layer of Carbosil (200 μL of 70 mg/mL), 2) copper layer (100 μL of 0, 1, 3 wt% Cu particles in 50 mg/mL Carbosil), 3) a top coat of 50 μL of 50 mg/mL Carbosil. The ratio of the copper layer to top coat was done 2:1 as to mimic the number of dip coats used for film based studies. For NO-releasing samples, 10 wt% SNAP in the Carbosil base layer was used; a total of n=16 samples were used for each material. The wells were dried for 6 hours between coats, followed by 24 hours drying under vacuum to ensure all THF had been removed from the wells.

Exposure to the PRP solution was done using 300 μL of the calcified PRP and incubated at 37°C for 2 hours with mild rocking (25 rpm) on a Medicus Health blood tube rocker. Following the incubation, the wells were infinitely diluted with 10 mM PBS. Lysing of the adhered cells was done using 200 μL Triton-PBS buffer (2% v/v Triton-X-100 in PBS). Briefly, 100 μL of the lysing buffer for each sample was combined with 100 μL of the detection agent and incubated for 25 min protected from light. A calibration curve was constructed using known dilutions of the final PRP, and the platelet adhesion on the polymeric composite was determined. The absorbance of each well was then measured using a 96 well plate reader (Biotek), and the number of platelets adhered was determined using the calibration curve. All protocols pertaining to the use of whole blood and platelets were approved by the University of Georgia.

2.2.6 In vitro analysis of inhibition of bacterial adhesion on polymer surface

—In order to evaluate the effectiveness of copper, nanoparticle assisted NO release from SNAP as a potent antibacterial strategy, a modified version of standard bacterial adhesion test was performed.[52] Antibacterial activity of the Cu-SNAP composites was investigated using common causative agents of blood infections: gram-positive *Staphylococcus aureus* (*S. aureus*) and gram-negative *Pseudomonas aeruginosa* (*P. aeruginosa*). These bacteria are among the most common causes of nosocomial bloodstream infection that can form embedded biofilm matrices on indwelling biomedical devices.[53] To investigate the antibacterial attribute of the fabricated films, single isolated colonies of *P. aeruginosa* and *S. aureus* strains were obtained from pre-culture LB agar Petri dishes, inoculated in 5 mL of LB medium, and incubated for 14 h at 120 rpm and 37°C. To ensure that the bacteria was in actively dividing phase, the optical density of the culture was measured at 600 nm ($O.D_{600}$) using UV-vis spectrophotometer (Thermo scientific Genesys 10S UV-Vis). To wash off the traces of the LB medium, the culture was centrifuged for 8 min at 2500 rpm, the supernatant was discarded, and an equivalent amount of sterile phosphate buffer saline (PBS, pH 7.4) was added and centrifuged again for 8 min at 2500 rpm. Fresh PBS was then added to the formed cell pellet and was vortexed for 30 secs to suspend the cells to be used in the study. The $O.D_{600}$ of the cell suspension in PBS was measured, using PBS as blank, and adjusted to get 10^8-10^{10} CFU/mL. Each of the test films (SNAP, 1 wt% Cu-NPs, 3 wt% Cu-NPs, 1 wt % Cu-SNAP, 3 wt% Cu-SNAP) and the control films (Carbosil) were exposed to 2 mL of *S. aureus* suspension and *P. aeruginosa* individually in 15 mL sterile tubes (n=3). This was followed by incubating the films at 37 °C for 24 h at a shaking speed of 120 rpm. After 24 h films were taken out of suspended bacterial culture and rinsed with sterile PBS to remove any loosely bound bacteria. To ensure that all the bound bacteria are detached from the films, the films were transferred to 2 mL of fresh PBS, sonicated with Omni-TH sonicator for 1 min followed by 30 s of vortex mixing. The resulting bacterial suspension was serially diluted (10^{-1} to 10^{-5}) and plated in Petri dishes with LB agar medium and incubated at 37 °C for 24 h. Post incubation, the CFUs were counted and the attached viable CFU per surface area (cm^2) of the films were compared to the control and test films. The CFU per surface area of the films were counted and compared with controls to evaluate their efficacy to inhibition bacterial adhesion on the surface of the films. All protocols pertaining to the use of bacterial strains were used in a BSL-2 facility approved by the University of Georgia.

$$\%\ Bacterial\ inhibition = \frac{\left(\frac{CFU}{cm^2}\ in\ control\ samples - \frac{CFU}{cm^2}\ in\ test\ samples\right) \times 100}{\frac{CFU}{cm^2}\ in\ control\ samples}$$

2.2.7 Cu leaching studies using Inductively Coupled Plasma Mass Spectroscopy (ICP-MS)—

Inductively coupled plasma mass spectrometry (ICP-MS) is an ultra-sensitive method for the detection of specific elements. A VG ICP-MS Plasma Quad 3 instrument was used to detect the exact concentration of copper in sample leachates. The polymeric films with Cu-NPs (1 wt% Cu-NPs, 3 wt% NPs, 1 wt% Cu-SNAP and 3 wt% Cu-SNAP) were tested for potential copper diffusion. To obtain the leachate, 10 mg of the polymer films were soaked in 10 mL DMEM medium (concentration 1 mg per mL of medium) for 24 hours. Thereafter, the films were removed and the medium was tested for leached ^{65}Cu isotope following a previously established protocol.[54]

2.2.8 In vitro cytotoxicity assay—

The cytotoxicity study was conducted to demonstrate any potential leaching from Cu-Carbosil, SNAP and Cu-SNAP film and its toxic effects on 3T3 mouse fibroblast cell line (ATCC-1658) in accordance with the ISO 10993 standard. The manufacturer's (Sigma-Aldrich) protocol was followed while using the Cell Counting Kit-8 (CCK-8) which utilizes highly water-soluble tetrazolium salt. WST-8 [2-(2-methoxy-4-nitrophenyl)-3-(4-nitrophenyl)-5-(2,4-disulfophenyl)-2H-tetrazolium monosodium salt] is reduced by dehydrogenases in live cells to give formazan (an orange color product) detected at 450 nm. Thus, the number of living cells is directly proportional to the amount of the formazan dye generated by dehydrogenases in cells. The detection sensitivity of CCK-8 solution is higher than other tetrazolium salts such as MTT, MTS, XTT or WST-1 and unlike MTT it does not require the killing of cells for the assay. All protocols pertaining to the use of mammalian cells were approved by the University of Georgia

Cell culture: Mouse fibroblast cells were cultured in 75 cm^2 T-flask DMEM medium with 4.5g/L glucose and L-glutamine, 10% fetal bovine serum (FBS) and 1% penicillin-streptomycin and incubated at 37°C in a humidified atmosphere with 5% CO_2. After the confluency reached 90%, the cells were trypsinized (0.18% trypsin and 5 mM EDTA) and 5000 cell/mL were seeded in 96 well plates.

Preparation of leachates: The polymeric films were allowed to leach in the DMEM medium by following the ISO standards (ISO 10993–5:2009 Test for in vitro cytotoxicity) to collect the extract (if any). Extracts from control and test films were obtained by soaking 10 mg of the sterilized films in 10 mL DMEM medium (concentration of 1 mg/mL of medium) in an amber color vials (to prevent NO release by light stimulation) and incubated for 24 h at 37°C. After 24 h, the films were removed and the resulting extracts were kept in the refrigerator (4°C) prior to using them in the cell culture experiment.

Determination of degree of cytotoxicity: The suspension of cultured cells (5000 cell/mL) was inoculated (100 μL/well) in a 96-well plate. The 96-well plate was then pre-incubated in a humidified incubator at 37°C, 5% CO_2 for 24 h. After 24 h, 10 μL of the different

leachates were added (n=5) and incubated for another 24 h to allow the potential toxicants to act on cells. To each of the wells, 10 μL of the CCK-8 solution was added and incubated for 3 h. To avoid the background interference, 100 μL of the DMEM medium was added in 4 of the wells. The absorbance was measured at 450 nm and compared to cells grown in the leachate containing culture. Results were reported as percentage cell viability (percentage of control) after subtracting the average absorbance of the medium (without cells) as follows.

$$\%\,Cell\,Viability = \frac{\text{Absorbance of the test samples}}{\text{Absorbance of the control samples}} \times 100$$

2.2.9 Statistical analysis—All data is reported as a mean ± standard deviation. All statistical comparisons were done using standard two-*tailed t*-test with unequal variance. The significance is stated for comparisons with $p < 0.05$.

3. Results and Discussion

3.1 NO flux analysis

As demonstrated in Figure 1, the NO release from the SNAP containing polymeric composites was enhanced by applying two layers of copper nanoparticles (Cu-NPs) and finally top-coated with Carbosil to prevent leaching of Cu-NPs and SNAP. The NO release mechanism involves oxidation of Cu^0 nanoparticles to Cu^{2+} ions in the presence of moisture. The resulting Cu^{2+} ions reduce to the active species, Cu^+ ions in the presence of reducing agents like thiolates (RS^-) that exist in the physiological environment (Figure 2).

Ultimately, the Cu^+ ions catalyze the generation of NO from RSNOs such as SNAP.[13, 55] The NO flux from the SNAP films with and without Cu-NPs was measured using Nitric oxide analyzer (NOA) at different time points. Thiolate stability and formation at physiological pH has been investigated in an earlier study by D. Lyn. H. Williams.[56] Theoretically, all the buffers (including PBS, DMEM, and blood) when properly adjusted to a pH of 7.4, will produce similar NO release via the previously discussed reaction mechanism (Figure 2).

The addition of Cu-NPs catalytically increased the generation of NO from the polymer films (Figure 3). Polymer films containing 10% SNAP had a flux of $1.32 \pm 0.6 \times 10^{-10}$ mol^{-2} min^{-1}, which agrees with previously reported release rates.[42, 45–46, 57] Films containing 1 wt% Cu-SNAP and 3 wt% Cu-SNAP had increased flux values of $4.48 \pm 0.5 \times 10^{-10}$ $mol^{-2}min^{-1}$ and $4.84 \pm 0.3 \times 10^{-10}$ $mol^{-2}min^{-1}$, respectively. This NO flux corresponds to the higher end of physiological levels of NO released by endothelial cells that line the blood vessels. Incorporation of 5 wt% Cu-NPs in the SNAP films showed a drastic increase in the NO-release ($11.7 \pm 3.6 \times 10^{-10}$ mol min^{-1} cm^{-2}) from these materials was almost two times higher than the physiological levels, and therefore not used in the following *in vitro* studies. While the release of NO from 1 wt% and 3 wt% Cu-NPs films are similar initially, 3 wt% films sustained a higher release rate over the first 24-hour period. Films containing 5 wt% Cu-NPs showed similar release rates to those containing 3 wt% Cu after the first 24-hour period. These results demonstrate that the optimal concentration of Cu-NPs in the polymeric

NO releasing composites presented in this study lies between 0–3 wt% for physiological release rates. Higher Cu-NPs concentrations, however, can provide increased NO fluxes well within physiological limits after 24 h. The decrease in NO flux for all composition can theoretically be explained on the basis of the ability of the Cu^{2+} to be reduced back to Cu^{1+} which acts as the ultimate catalyst enhancing NO release from SNAP, as Cu^{2+} does not contribute to the catalytic release of NO.[58] Initially, the films contain both crystallized regions of SNAP, as well as SNAP that is homogeneously incorporated within the polymer matrix.[59] This combination of monodisperse SNAP and crystallized regions contribute to the higher initial release rates of NO, followed by extended release rates that can be maintained for > 20 d.[40] The initial state of the composites allows for SNAP and Cu-NPs within the film to have minimum separation, leading to the reactive species (RS^-) being readily available for the reduction of Cu^{2+} to Cu^{1+}, where the catalytic activity can be maintained. Once SNAP from the homogenous region is depleted and NO release is only from the crystallized regions, the catalytic ability of Cu ions to continue NO release can be limited by diffusion of Cu^{2+} to the crystallized regions to be reduced by the free thiols. Therefore, increasing the concentration of Cu-NPs will increase the available Cu^{2+} ions to diffusion to these crystallized regions, which is observed in the 24-hour measurements. In the past, when used *in vivo*, we demonstrated that polymeric materials with incorporated NO donors could achieve higher levels of NO release due to the availability of free ascorbic acid in the blood to reduce Cu^{2+} to Cu^{1+},[60–61] and could provide NO release from systemic RSNOs as well.[13] Control over this reduction reaction would result in lower concentrations of Cu-NPs required in the films to sustain increased NO release while lowering the initial release rate.

3.2 Surface morphology analysis of copper coats on polymeric composites

Surface morphology is an important parameter to decide the translational success of an antimicrobial polymer for medical application as surface morphologies can alter blood protein and bacterial adhesion on the surface of the polymer. No significant Cu-NPs traces were found on film's surface with 3 wt% copper observed as illustrated by the images captured from Surface Electron Microscopy (SEM) at an accelerating voltage of 5 kV. At a magnification of 225X, the surface of carbosil control looked very similar to the Surface with 3 wt% Cu-NPs. This assures that the presence of a top coat of the Cu-NPs does not alter surface morphology of the polymeric composite (Figure 4).

3.3 Detection of copper leaching

Detection of the amount of copper leaching from the polymeric composites is crucial for the preclinical success of biomaterial since a high diffusion of copper ions from the polymers will highly influence cell cytotoxicity and bacterial adhesion studies. After 24 h of soaking 10 mg of the polymer films in 5 mL DMEM medium (concentration 2 mg per mL of medium) to allow any potential leaching, the standard ICP-MS method was performed to monitor copper leaching from the films. The results of the detected copper leaching are shown in Table 1. The Cu-SNAP films showed a slightly higher amount of leached copper than films only containing Cu-NPs but still much below the recommended limit. The increase for the Cu-SNAP films is most likely due to the formation of nitric acid from the conversion of NO to nitrites within the medium.[62] Copper is known to be highly soluble in nitric acid, so the presence of even trace amounts could dissolve a portion of the copper

within the polymer matrix. The highest recorded levels (306.9 ± 99.5 ppb) from the films leachate in this study were well below cytotoxic concentrations towards mammalian cells. Earlier *in vitro* reports on copper cytotoxicity on a variety of mammalian cell lines have shown that cell viability stays at 100% until the concentration of copper reaches approximately 1000 ppb.[63–65] In a previous study, 10 wt% of copper nanoparticles have been blended within blood contacting polymers that demonstrated the negligible amount of leaching.[13] This demonstrates even further the negligible amount of copper being leached into the medium and its innocuous impact on biocompatibility.

3.4 Effects of Cu/SNAP on platelet adhesion

Many blood contacting devices such as vascular catheters have issues with blood compatibility due to the formation of a blood clot on device surface after implantation, therefore, the ability of a biomaterial to prevent platelet adhesion is an important parameter to validate the hemocompatibility. The ability for Cu-NPs incorporating SNAP films to prevent platelet adhesion was determined using an LDH assay after exposure to porcine platelet rich plasma (PRP) for 2 h. Freshly drawn porcine blood was drawn 9:1 into 3.4% sodium citrate and processed to give a final recalcified platelet-rich solution with a total platelet count ca. 2×10^8 platelets/mL as described in methods section 2.2.5. Total platelet adhesion to each composite composition is shown in Figure 5. The combination of 10 wt% SNAP with 3 wt% Cu nanoparticles (3% Cu-SNAP) provides the largest decrease in platelet adhesion, showing a 92% reduction when compared to Carbosil controls. This is expected as the combination of SNAP with 3 wt% Cu particles provided the highest level of NO release ($p = 0.003$). Similarly, as the little difference was observed between 1 wt% Cu-SNAP films and 3 wt% Cu-SNAP films in NO release, insignificant changes in the platelet adhesion was observed. However, the higher level of NO release provided by the 3 wt% Cu composite was observed to have slightly decreased platelet adhesion. The presence of Cu particles alone provides significant reduction in platelet adhesion when compared to Cu-Carbosil controls without SNAP (1 wt% Cu-Carbosil: 72% reduction, $p = 0.006$; 3 wt% Cu-Carbosil: 82% reduction, $p = 0.003$). The ability for low levels of NO generated by the reaction of the endogenous RSNOs present in the plasma (10 μM) with Cu-NPs demonstrate that while low levels of NO can reduce platelet adhesion drastically (>70%), the release of NO at the upper limit of the physiological release rates does significantly reduce platelet activation and adhesion when compared to lower levels of NO release.

The ability for the Cu assisted the generation of NO from natural RSNOs has been shown *in vivo*, reducing thrombus formation in a rabbit extracorporeal circuit model after 4 h ca. 40%.[13] Larger reductions in platelet adhesion seen in this study may result from using PRP, while the previous work was conducted *in vivo*, where hemoglobin present in the red blood cells may bind to NO, limiting the efficacy to prevent platelet adhesion. While Cu particle size for generation of NO from natural RSNOs has yet to be optimized, the focus of this work was to provide catalytic control of NO released from blended RSNOs within the polymer film, and not the generation of NO from naturally occurring RSNOs within the blood. However, this result shows that while the physical blending of NO donors into polymeric materials is limited in the lifetime of the NO release, the NO generating capability of the Cu ions within the polymer can continue to provide activity to prevent the adhesion of platelets to the

material surface, providing controlled and predictable release rates from both regimes (NOrel and NOgen), making this material ideal for longer term blood contacting devices such as vascular catheters.

3.5 Inhibition of gram positive and negative bacteria adhesion on polymer surface

Biomedical device related infections (BDRIs) are one of the major cause of morbidity and the associated healthcare cost. The gram-positive *S. aureus* and gram-negative *P. aeruginous* are among the most common causative agents of hospital acquired infections.[65] *Invitro* bacteria, testing demonstrates that the Cu-NPs assisted NO release is effective in reducing the population of viable bacterial cells on polymeric films against both grams positive and negative bacteria (Figure 6). Even individually NO donor (SNAP), as well as Cu-NP controls, inhibited both gram positive and gram negative bacteria. The antibacterial properties of copper are due to its oligodynamic effect while the bactericidal properties of NO are due to denaturation of enzymes, deamination of DNA and lipid oxidation in pathogens.[32] In the presence of Cu-NPs coats the catalytic activity of copper increase the NO release from the SNAP thus enhancing the bacterial inhibition as compared to SNAP films alone. The NO flux release was directly proportional to the amount of Cu-NPs present and hence more bacteria-killing on the surface of the film. Table 2 shows the bacterial colony forming units per surface area of the composite (CFU/cm^2) that were present on the surface of each of the films. The NO flux is inversely proportional to the bacterial CFU/cm^2 showing that the enhanced NO release by Cu-SNAP films inhibited the bacterial growth significantly. Overall there was a marked reduction of up to 2 logs by SNAP films while Cu-NPs coated films showed bacterial inhibition up to 5 logs. Among all the tested films, the 3wt% Cu-SNAP films with allowed the least amount of bacterial colony forming to grow per unit surface area of the composite (CFU/cm^2) as shown in Figure 6. The observed difference between the antibacterial effect of NO on gram-negative and gram-positive bacteria can be attributed to differences in their cell membrane properties. In the presence of Cu-NPs coats, the catalytic activity of copper increases the NO release from SNAP thus enhancing the bacterial inhibition as compared to the SNAP films alone. Table 2 shows a comparative quantification of the bacterial colony forming units per surface area of the composite (CFU/cm^2) that were present on the surface of each type of the films. The NO flux is inversely proportional to the bacterial CFU/cm^2 showing that the enhanced NO release by Cu-SNAP films inhibited the bacterial growth significantly.

This is evident from the results that the higher NO flux can result in the better bacterial inhibition as compared to the controls. In a biofilm, the antibiotic resistant bacteria can encase themselves in a hydrated matrix of polysaccharide and protein thus defending themselves effectively against the action of antibiotics.[11, 66] The low molecular weight of NO allows penetrating through the matrix in the biofilm which gives it an extra advantage over antibiotics and silver-based antibacterial strategies.[67–68] Having higher influx of NO allows a higher penetration of the NO through the biofilm and thus killing the bacteria with comparatively significantly lesser dose in situations where other antibacterials are mostly ineffective. Furthermore, the use of NO is unlikely to stimulate the production of resistant strains due to rapid reduction of microbial load.[26, 33–34] In the past, we have shown the antibacterial attributes of NO releasing membrane against *A.baumanni*, *S. aureus*, *E. coli*, *L.*

monocytogenes, and E. faecalis.[30–42] In addition, other published reports have also shown a significant reduction in bacterial growth (1–24 h studies) owing to the antibacterial properties of NO.[24, 27, 29] However, these studies have reported the effect of bacterial exposure on NO flux profile. Hence NO release was also measured from films after the bacterial studies to confirm NO was still being released from the residual SNAP in the films. The results showed that the residual NO flux after the bacterial exposure was still maintained within the physiological levels demonstrating that these films can be used beyond 24 h to kill bacteria if needed (Figure 7). As Cu-NPs has also been demonstrated to provide antibacterial properties, further optimization can be done to not only tune the NO release for the specific application but also provide the highest antibacterial activity between the level of Cu and NO release.

3.5 Cytotoxicity of polymeric films leachates

As per the ISO 10993 standards, the purpose of performing biocompatibility testing of the medical device is to investigate its undesirable physiological effects such as cytotoxicity and to validate its fitness for human use. Recent studies have shown NO releasing strategies to be highly effective for controlling bacterial infection but the NO flux was much higher than the upper range of physiological NO flux.[69] Although antibacterial characteristic and platelet inactivation are one of the most important parameters for developing medical devices, it should not be at the cost of the host mammalian cells due to cytotoxicity. Hence achieving maximum bacterial inhibition and platelet activation while ensuring that these NO releasing composites are not toxic to mammalian cells was another important objective of the present study. In the present study, we evaluated the relative cytotoxicity of potential leachates from the films with SNAP and/or Cu-NPs with respect to the control Carbosil films using cell counting kit-8 (CCK-8) assay after soaking the films in the medium for 24 h. The number of viable cells in the composites with SNAP, 1 wt%, and 3 wt% Cu-NPs are very similar relative to the control Carbosil composites demonstrating that these composites are biocompatible to the mammalian fibroblast cells (Figure 8). Morphologically, the fibroblast cells maintained their regular dendritic shapes as demonstrated by optical images obtained at 10X magnification using EVOS XL microscope (Figure 9). These results are in line with the Cu leachate detection analysis (Section 3.3) which demonstrated the negligible amount of copper (306.9 ppb) in the leachates from films, which is much below the recommended safety limit (2000 ppb) by the WHO. Furthermore, any leaching of SNAP, or more likely NAP (N-acetyl-penicillamine) and possibly dimers of NAP, would ultimately hydrolyze to penicillamine (and acetic acid). Low level of penicillamine (FDA approved) is widely used for heavy metal poising in humans as per FDA recommendation.[37] The NO flux exhibited by the endothelial cells in the blood vessels lining is in the range of 0.5–4.0 × 10^{-10} mol min^{-1} cm^{-2} [20] Theoretically, a flux closer to physiological range should not exhibit a cytotoxic response to the host. cells. The NO flux released by 1 wt% Cu-SNAP and 3% Cu-SNAP were reported to be very close to the upper range of endogenous NO flux, i.e 4.48 ± 0.5 × 10^{-10}, 4.8 4± 0.3 × 10^{-10} mol min^{-1} cm^{-2} respectively, and hence justify the absence of cytotoxicity by the polymeric films as a response to SNAP or its by-products leaching (if any) in the medium. In the past, polymeric films with 10 wt% SNAP are shown to be hemocompatible and biocompatible with mammalian cells.[44, 70] Overall this *in vitro* study showed these NO releasing polymeric composite containing 1 wt% or 3 wt% Cu-NPs

in combination with 10% SNAP are safe towards mammalian cells through the negligible amount of leaching. Further testing in animal models would be helpful to establish *in vivo* data to reconfirm the efficacy of these composite in pre-clinical settings.

4. Conclusions

Due to the dose-dependent effect of NO, achieving a local and continuous release of NO from the biomedical implants is a desirable attribute for their clinical success. In this study, controlled NO release from SNAP containing Carbosil films was achieved by incorporating Cu-NPs coatings on the SNAP films. Concentrations of Cu-NPs above 3 wt% were found to increase the release rate of NO from the polymer above physiological levels. While the SNAP films exhibit a NO flux of $1.32 \pm 0.6 \times 10^{-10}$ mol min^{-1} cm^{-2}, utilizing the Cu-NPs increases the NO release up to $4.84 \pm 0.3 \times 10^{-10}$ due to the catalytic activity of copper. This resulted in significant reduction (up to 5 logs) in bacterial growth on the polymer surface. The Cu-SNAP combination could prevent >92% of platelet adhesion upon exposure to porcine PRP for 2 h. The ICP-MS study showed that the leaching of copper from these films is below toxicity limit. Furthermore, the Cu-SNAP combination was found to be non-cytotoxic to mammalian cells as demonstrated by the cytotoxicity assay performed on the mouse fibroblast 3T3 cell line. Overall the leaching and cytotoxicity studies combinedly provide evidence that these treatments may be safe for clinical use. Overall, when compared with the conventional approaches, the study recommends that the Cu-SNAP composites can provide an increased antibacterial activity for biomedical device coatings without causing drug resistance and cytotoxicity associated with currently available antimicrobial agents. The amount of NO release can be tuned by varying the copper concentration, thus expanding the use of Cu-SNAP combination for multiple biomedical applications. Overall, these composites are exceptionally promising to fabricate a new generation of medical devices with controlled NO release, reduced platelet adhesion and superior degree of microbial inhibition with potential biocompatibility.

Acknowledgements

Funding for this work was supported by National Institutes of Health, USA grants K25HL111213, R01HL134899, and Centers for Disease Control and Prevention contract 200-2016-91933.

References

(1). Grahn B; Wilson P; Krepel C; Seabrook G; Johnson C; Edmiston C Biomedical Device-Associated Infections in Surgical-Critical Care Patients. Am. J. Infect. Control 2004, 32 (3), E33–E34.

(2). Welsh CA; Flanagan ME; Hoke SC; Doebbeling BN; Herwaldt L Reducing Health Care-Associated Infections (Hais): Lessons Learned from a National Collaborative of Regional Hai Programs. Am. J. Infect. Control 2012, 40 (1), 29–34. [PubMed: 21775022]

(3). Donlan RM Biofilm Formation: A Clinically Relevant Microbiological Process. Clin. Infect. Dis 2001, 33 (8), 1387–1392. [PubMed: 11565080]

(4). O'gara JP; Humphreys H Staphylococcus Epidermidis Biofilms: Importance and Implications. J. Med. Microbiol 2001, 50 (7), 582–587. [PubMed: 11444767]

(5). O'gara JP Ica and Beyond: Biofilm Mechanisms and Regulation in Staphylococcus Epidermidis and Staphylococcus Aureus. FEMS Microbiol. Lett 2007, 270 (2), 179–188. [PubMed: 17419768]

(6). Lee Y-H; Cheng F-Y; Chiu H-W; Tsai J-C; Fang C-Y; Chen C-W; Wang Y-J Cytotoxicity, Oxidative Stress, Apoptosis and the Autophagic Effects of Silver Nanoparticles in Mouse Embryonic Fibroblasts. Biomaterials 2014, 35 (16), 4706–4715. [PubMed: 24630838]

(7). Park E-J; Yi J; Kim Y; Choi K; Park K Silver Nanoparticles Induce Cytotoxicity by a Trojan-Horse Type Mechanism. Toxicol. In Vitro 2010, 24 (3), 872–878. [PubMed: 19969064]

(8). Baldi C; Minoia C; Di Nucci A; Capodaglio E; Manzo L Effects of Silver in Isolated Rat Hepatocytes. Toxicol. Lett 1988, 41 (3), 261–268. [PubMed: 3376153]

(9). Asharani PV, Mun GLK, Hande MP, Valiyaveettil. Cytotoxicity and Genotoxicity of Silver Nanoparticles in Human Cells. ACS Nano 2009, 3 (2), 279–290. [PubMed: 19236062]

(10). Cheng X, Zhang W, Ji Y, Meng J, Guo H, Liu J, Wu X, Xu H Revealing Silver Cytotoxicity Using Au Nanorods/Ag Shell Nanostructures: Disrupting Cell Membrane and Causing Apoptosis through Oxidative Damage. RSC Advances 2013, 3 (7), 2296–2305.

(11). Stewart PS; Costerton JW Antibiotic Resistance of Bacteria in Biofilms. The lancet 2001, 358 (9276), 135–138.

(12). Davies J Inactivation of Antibiotics and the Dissemination of Resistance Genes. Science 1994, 264 (5157), 375–382. [PubMed: 8153624]

(13). Major TC; Brant DO; Burney CP; Amoako KA; Annich GM; Meyerhoff ME; Handa H; Bartlett RH The Hemocompatibility of a Nitric Oxide Generating Polymer That Catalyzes S-Nitrosothiol Decomposition in an Extracorporeal Circulation Model. Biomaterials 2011, 32 (26), 5957–5969. [PubMed: 21696821]

(14). Brisbois EJ; Major TC; Goudie MJ; Meyerhoff ME; Bartlett RH; Handa H Attenuation of Thrombosis and Bacterial Infection Using Dual Function Nitric Oxide Releasing Central Venous Catheters in a 9day Rabbit Model. Acta Biomater. 2016, 44, 304–312. [PubMed: 27506125]

(15). Robinson TM; Kickler TS; Walker LK; Ness P; Bell W Effect of Extracorporeal Membrane Oxygenation on Platelets in Newborns. Crit. Care Med 1993, 21 (7), 1029–1034. [PubMed: 8319460]

(16). Dillon PA; Foglia RP Complications Associated with an Implantable Vascular Access Device. J. Pediatr. Surg 2006, 41 (9), 1582–1587. [PubMed: 16952595]

(17). Ziche M; Morbidelli L Nitric Oxide and Angiogenesis. J. Neurooncol 2000, 50 (1), 139–148. [PubMed: 11245273]

(18). Dimmeler S; Fleming I; Fisslthaler B; Hermann C; Busse R; Zeiher AM Activation of Nitric Oxide Synthase in Endothelial Cells by Akt-Dependent Phosphorylation. Nature 1999, 399 (6736), 601–605. [PubMed: 10376603]

(19). Villalobo A Nitric Oxide and Cell Proliferation. The FEBS journal 2006, 273 (11), 2329–2344. [PubMed: 16704409]

(20). Vaughn MW; Kuo L; Liao JC Estimation of Nitric Oxide Production and Reactionrates in Tissue by Use of a Mathematical Model. Am. J. Physiol.: Heart Circ. Physiol 1998, 274 (6), H2163–H2176.

(21). Vodovotz Y; Bogdan C; Paik J; Xie Q; Nathan C Mechanisms of Suppression of Macrophage Nitric Oxide Release by Transforming Growth Factor Beta. J. Exp. Med 1993, 178 (2), 605–613. [PubMed: 7688028]

(22). Hibbs JB; Taintor RR; Vavrin Z; Rachlin EM Nitric Oxide: A Cytotoxic Activated Macrophage Effector Molecule. Biochem. Biophys. Res. Commun 1988, 157 (1), 87–94. [PubMed: 3196352]

(23). Macmicking J; Xie Q-W; Nathan C Nitric Oxide and Macrophage Function. Annu. Rev. Immunol 1997, 15 (1), 323–350. [PubMed: 9143691]

(24). Charville GW; Hetrick EM; Geer CB; Schoenfisch MH Reduced Bacterial Adhesion to Fibrinogen-Coated Substrates Via Nitric Oxide Release. Biomaterials 2008, 29 (30), 4039–4044. [PubMed: 18657857]

(25). Cai W; Wu J; Xi C; Meyerhoff ME Diazeniumdiolate-Doped Poly(Lactic-Co-Glycolic Acid)-Based Nitric Oxide Releasing Films as Antibiofilm Coatings. Biomaterials 2012, 33 (32), 7933–7944. [PubMed: 22841918]

(26). Hetrick EM; Schoenfisch MH Antibacterial Nitric Oxide-Releasing Xerogels: Cell Viability and Parallel Plate Flow Cell Adhesion Studies. Biomaterials 2007, 28 (11), 1948–1956. [PubMed: 17240444]

(27). Engelsman AF; Krom BP; Busscher HJ; Van Dam GM; Ploeg RJ; Van Der Mei HC Antimicrobial Effects of an No-Releasing Poly (Ethylene Vinylacetate) Coating on Soft-Tissue Implants in Vitro and in a Murine Model. Acta Biomater 2009, 5 (6), 1905–1910. [PubMed: 19251498]

(28). Carlsson S; Weitzberg E; Wiklund P; Lundberg JO Intravesical Nitric Oxide Delivery for Prevention of Catheter-Associated Urinary Tract Infections. Antimicrob. Agents Chemother 2005, 49 (6), 2352–2355. [PubMed: 15917532]

(29). Mihu MR; Sandkovsky U; Han G; Friedman JM; Nosanchuk JD; Martinez LR The Use of Nitric Oxide Releasing Nanoparticles as a Treatment against Acinetobacter Baumannii in Wound Infections. Virulence 2010, 1 (2), 62–67. [PubMed: 21178416]

(30). Brisbois EJ; Bayliss J; Wu J; Major TC; Xi C; Wang SC; Bartlett RH; Handa H; Meyerhoff ME Optimized Polymeric Film-Based Nitric Oxide Delivery Inhibits Bacterial Growth in a Mouse Burn Wound Model. Acta Biomater. 2014, 10 (10), 4136–4142. [PubMed: 24980058]

(31). Sundaram J; Pant J; Goudie MJ; Mani S; Handa H Antimicrobial and Physicochemical Characterization of Biodegradable, Nitric Oxide-Releasing Nanocellulose–Chitosan Packaging Membranes. J. Agric. Food Chem 2016, 64 (25), 5260–5266. [PubMed: 27258235]

(32). Fang FC Perspectives Series: Host/Pathogen Interactions. Mechanisms of Nitric Oxide-Related Antimicrobial Activity. J. Clin. Invest 1997, 99 (12), 2818. [PubMed: 9185502]

(33). Feelisch M The Use of Nitric Oxide Donors in Pharmacological Studies. Naunyn-Schmiedeberg's Arch. Pharmacol 1998, 358 (1), 113–122. [PubMed: 9721012]

(34). Bogdan C Nitric Oxide and the Immune Response. Nat. Immunol 2001, 2 (10), 907–916. [PubMed: 11577346]

(35). Frost MC, Reynolds MM, Meyerhoff ME Polymers Incorporating Nitric Oxide Releasing/ Generating Substances for Improved Biocompatibility of Blood-Contacting Medical Devices. Biomaterials 2005, 26 (14), 1685–1693. [PubMed: 15576142]

(36). Riccio DA; Schoenfisch MH Nitric Oxide Release: Part I. Macromolecular Scaffolds. Chem. Soc. Rev 2012, 41 (10), 3731–3741. [PubMed: 22362355]

(37). Carpenter AW; Schoenfisch MH Nitric Oxide Release: Part Ii. Therapeutic Applications. Chem. Soc. Rev 2012, 41 (10), 3742–3752. [PubMed: 22362384]

(38). Frost MC; Reynolds MM; Meyerhoff ME Polymers Incorporating Nitric Oxide Releasing/ Generating Substances for Improved Biocompatibility of Blood-Contacting Medical Devices. Biomaterials 2005, 26 (14), 1685–1693. [PubMed: 15576142]

(39). Mccarthy CW; Guillory RJ; Goldman J; Frost MC Transition-Metal-Mediated Release of Nitric Oxide (No) from S-Nitroso-N-Acetyl-D-Penicillamine (Snap): Potential Applications for Endogenous Release of No at the Surface of Stents Via Corrosion Products. ACS Appl. Mater. Interfaces 2016, 8 (16), 10128–10135. [PubMed: 27031652]

(40). Brisbois EJ; Handa H; Major TC; Bartlett RH; Meyerhoff ME Long-Term Nitric Oxide Release and Elevated Temperature Stability with S-Nitroso-N-Acetylpenicillamine (Snap)-Doped Elast-Eon E2as Polymer. Biomaterials 2013, 34 (28), 6957–6966. [PubMed: 23777908]

(41). Reynolds MM; Hrabie JA; Oh BK; Politis JK; Citro ML; Keefer LK; Meyerhoff ME Nitric Oxide Releasing Polyurethanes with Covalently Linked Diazeniumdiolated Secondary Amines. Biomacromolecules 2006, 7 (3), 987–994. [PubMed: 16529441]

(42). Sundaram J; Pant J; Goudie MJ; Mani S; Handa H Antimicrobial and Physicochemical Characterization of Biodegradable, Nitric Oxide-Releasing Nanocellulose-Chitosan Packaging Membranes. J. Agric. Food Chem 2016.

(43). Brisbois EJ; Kim M; Wang X; Mohammed A; Major TC; Wu J; Brownstein J; Xi C; Handa H; Bartlett RH Improved Hemocompatibility of Multilumen Catheters Via Nitric Oxide (No) Release from S-Nitroso-N-Acetylpenicillamine (Snap) Composite Filled Lumen. ACS Appl. Mat. & Interfaces 2016, 8 (43), 29270–29279.

(44). Goudie MJ; Brisbois EJ; Pant J; Thompson A; Potkay JA; Handa H Characterization of an S-Nitroso-N-Acetylpenicillamine–Based Nitric Oxide Releasing Polymer from a Translational Perspective. International Journal of Polymeric Materials and Polymeric Biomaterials 2016, 65 (15), 769–778.

(45). Pant J; Goudie M; Brisbois E; Handa H Nitric Oxide-Releasing Polyurethanes. Advances in Polyurethane Biomaterials 2016, 417.

(46). Brisbois EJ; Davis RP; Jones AM; Major TC; Bartlett RH; Meyerhoff ME; Handa H Reduction in Thrombosis and Bacterial Adhesion with 7 Day Implantation of S-Nitroso-N-Acetylpenicillamine (Snap)-Doped Elast-Eon E2as Catheters in Sheep. J. Mater. Chem. B 2015, 3 (8), 1639–1645. [PubMed: 25685358]

(47). Stuehr DJ; Nathan C Nitric Oxide. A Macrophage Product Responsible for Cytostasis and Respiratory Inhibition in Tumor Target Cells. J. Exp. Med 1989, 169 (5), 1543–1555. [PubMed: 2497225]

(48). Palmer RM; Ferrige A; Moncada S Nitric Oxide Release Accounts for the Biological Activity of Endothelium-Derived Relaxing Factor. Nature 1987, 327 (6122), 524–526. [PubMed: 3495737]

(49). Frost MC; Meyerhoff ME Controlled Photoinitiated Release of Nitric Oxide from Polymer Films Containing S-Nitroso-N-Acetyl-Dl-Penicillamine Derivatized Fumed Silica Filler. J. Am. Chem. Soc 2004, 126 (5), 1348–1349. [PubMed: 14759186]

(50). Flinn FB; Inouye J Some Physiological Aspects of Copper in the Organism. J. Biol. Chem 1929, 84 (1), 101–114.

(51). Chipinda I; Simoyi RH Formation and Stability of a Nitric Oxide Donor: S-Nitroso-N-Acetylpenicillamine. The Journal of Physical Chemistry B 2006, 110 (10), 5052–5061. [PubMed: 16526748]

(52). Torres N; Oh S; Appleford M; Dean DD; Jorgensen JH; Ong JL; Agrawal CM; Mani G Stability of Antibacterial Self-Assembled Monolayers on Hydroxyapatite. Acta Biomater. 2010, 6 (8), 3242–3255. [PubMed: 20188873]

(53). Otto M Staphylococcal Infections: Mechanisms of Biofilm Maturation and Detachment as Critical Determinants of Pathogenicity. Annu. Rev. Med 2013, 64, 175–188. [PubMed: 22906361]

(54). Vanhoe H; Vandecasteele C; Versieck J; Dams R Determination of Iron, Cobalt, Copper, Zinc, Rubidium, Molybdenum, and Cesium in Human Serum by Inductively Coupled Plasma Mass Spectrometry. Anal. Chem 1989, 61 (17), 1851–1857. [PubMed: 2802147]

(55). Williams DLH The Mechanism of Nitric Oxide Formation from S-Nitrosothiols (Thionitrites). Chem. Commun 1996, (10), 1085–1091.

(56). Williams DLH The Chemistry of S-Nitrosothiols. Acc. Chem. Res 1999, 32 (10), 869–876.

(57). Brisbois EJ; Kim M; Wang X; Mohammed A; Major TC; Wu J; Brownstein J; Xi C; Handa H; Bartlett RH Improved Hemocompatibility of Multi-Lumen Catheters Via Nitric Oxide (No) Release from S-Nitroso-N-Acetylpenicillamine (Snap) Composite Filled Lumen. ACS Appl. Mater. & Interfaces 2016.

(58). Harding JL; Reynolds MM Metal Organic Frameworks as Nitric Oxide Catalysts. J. Am. Chem. Soc 2012, 134 (7), 3330–3333. [PubMed: 22263610]

(59). Wo Y; Li Z; Brisbois EJ; Colletta A; Wu J; Major TC; Xi C; Bartlett RH; Matzger AJ; Meyerhoff ME Origin of Long-Term Storage Stability and Nitric Oxide Release Behavior of Carbosil Polymer Doped with S-Nitroso-N-Acetyl-D-Penicillamine. ACS Appl. Mater. Interfaces 2015, 7 (40), 22218–22227. [PubMed: 26393943]

(60). Oh BK; Meyerhoff ME Spontaneous Catalytic Generation of Nitric Oxide from S-Nitrosothiols at the Surface of Polymer Films Doped with Lipophilic Copper (Ii) Complex. J. Am. Chem. Soc 2003, 125 (32), 9552–9553. [PubMed: 12903997]

(61). Wonoputri V; Gunawan C; Liu S; Barraud N; Yee LH; Lim M; Amal R Copper Complex in Poly (Vinyl Chloride) as a Nitric Oxide-Generating Catalyst for the Control of Nitrifying Bacterial Biofilms. ACS Appl. Mater. Interfaces 2015, 7 (40), 22148–22156. [PubMed: 26418515]

(62). Squadrito GL; Pryor WA Oxidative Chemistry of Nitric Oxide: The Roles of Superoxide, Peroxynitrite, and Carbon Dioxide. Free Radical Biol. Med 1998, 25 (4), 392–403. [PubMed: 9741578]

(63). Fahmy B; Cormier SA Copper Oxide Nanoparticles Induce Oxidative Stress and Cytotoxicity in Airway Epithelial Cells. Toxicol. In Vitro 2009, 23 (7), 1365–1371. [PubMed: 19699289]

(64). Seth R; Yang S; Choi S; Sabean M; Roberts E In Vitro Assessment of Copper-Induced Toxicity in the Human Hepatoma Line, Hep G2. Toxicol. In Vitro 2004, 18 (4), 501–509. [PubMed: 15130608]

(65). Valodkar M; Rathore PS; Jadeja RN; Thounaojam M; Devkar RV; Thakore S Cytotoxicity Evaluation and Antimicrobial Studies of Starch Capped Water Soluble Copper Nanoparticles. J. Hazard. Mater 2012, 201, 244–249. [PubMed: 22178277]

(66). Costerton J; Stewart P Biofilms and Device-Related Infections. Persistent Bact. Infect 2000, 423–437.

(67). Barraud N; Hassett DJ; Hwang S-H; Rice SA; Kjelleberg S; Webb JS Involvement of Nitric Oxide in Biofilm Dispersal of Pseudomonas Aeruginosa. J. Bacteriol 2006, 188 (21), 7344–7353. [PubMed: 17050922]

(68). Hetrick EM; Shin JH; Paul HS; Schoenfisch MH Anti-Biofilm Efficacy of Nitric Oxide-Releasing Silica Nanoparticles. Biomaterials 2009, 30 (14), 2782–2789. [PubMed: 19233464]

(69). Pegalajar-Jurado A; Wold KA; Joslin JM; Neufeld BH; Arabea KA; Suazo LA; Mcdaniel SL; Bowen RA; Reynolds MM Nitric Oxide-Releasing Polysaccharide Derivative Exhibits 8-Log Reduction against Escherichia Coli, Acinetobacter Baumannii and Staphylococcus Aureus. J. Controlled Release 2015, 217, 228–234.

(70). Yapor J; Lutzke A; Pegalajar-Jurado A; Neufeld B; Damodaran V; Reynolds M Biodegradable Citrate-Based Polyesters with S-Nitrosothiol Functional Groups for Nitric Oxide Release. J. Mater. Chem. B 2015, 3 (48), 9233–9241. [PubMed: 32262922]

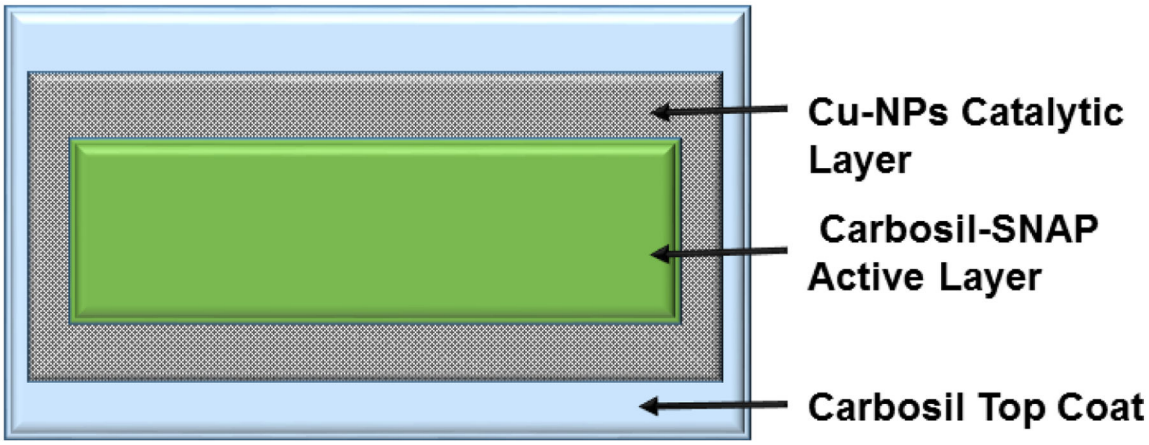

Figure 1.

A representative schematic of the polymeric composites with SNAP and copper nanoparticles (Cu-NPs) coating. The innermost active layer is made by incorporating 10 wt % SNAP in the CarboSil polymer. After completely drying the films, two coats of Cu-NPs (1, 3, or 5 wt%) blended in CarboSil were applied. A final top coat of CarboSil (50g/L) was layered to prevent leaching of SNAP and Cu-NPs.

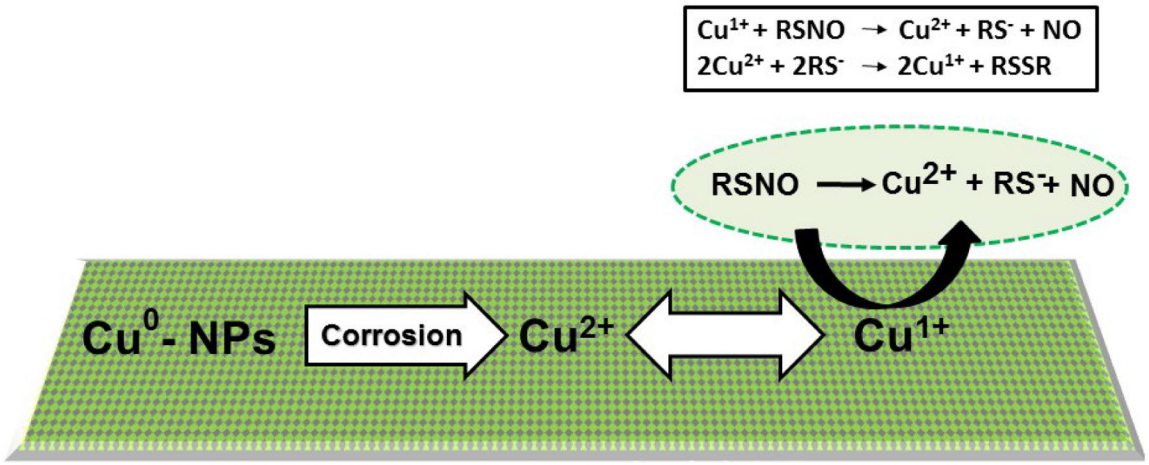

Figure 2.

The schematic representing the mechanism of nitric oxide (NO) release from an RSNO such as SNAP. The mechanism involves oxidation of Cu^0 nanoparticles to Cu^{2+} ions in the presence of water.

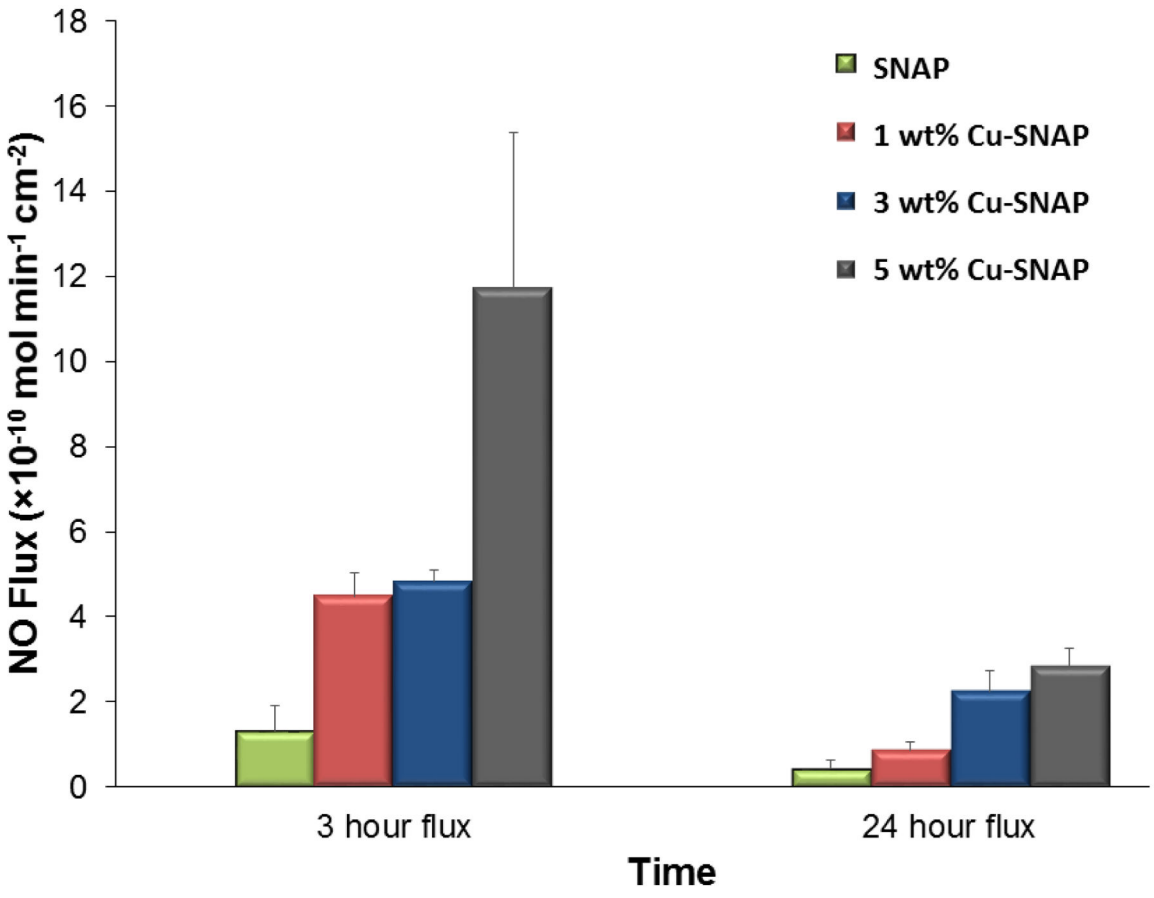

Figure 3.

Nitric oxide (NO) flux analysis of SNAP composites with or without copper nanoparticles (Cu-NPs) at different time points. As illustrated in the figure, there is a proportional increase in the NO flux release from the composites with increase in Cu-NPs concentration. The 1 wt % Cu-SNAP and 3 wt% Cu-SNAP films possess NO flux in the upper end of the physiological NO flux range while 5 wt% Cu-SNAP films showed almost two times NO flux than physiological range. P-values < 0.05 were used for comparison. The error bar represents standard deviation.

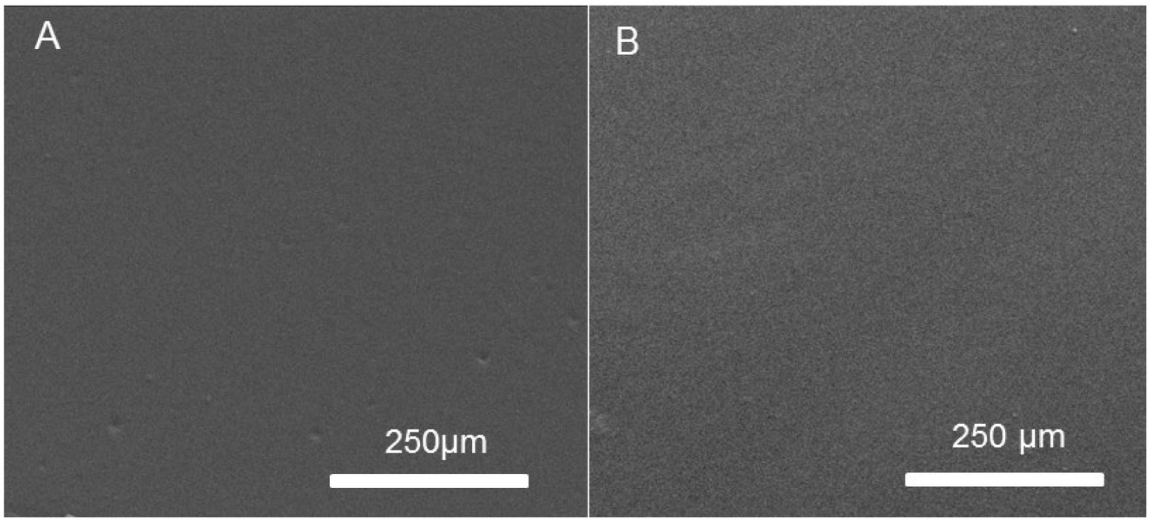

Figure 4.

Representative image of A) Carbosil (control) and B) Carbosil films with 3 wt% Cu-NPs taken at an accelerating voltage of 5 kV (225x magnification). Scale bar represents 250 microns. As depicted, the top layer of films with and without copper coats are similar in their surface morphologies.

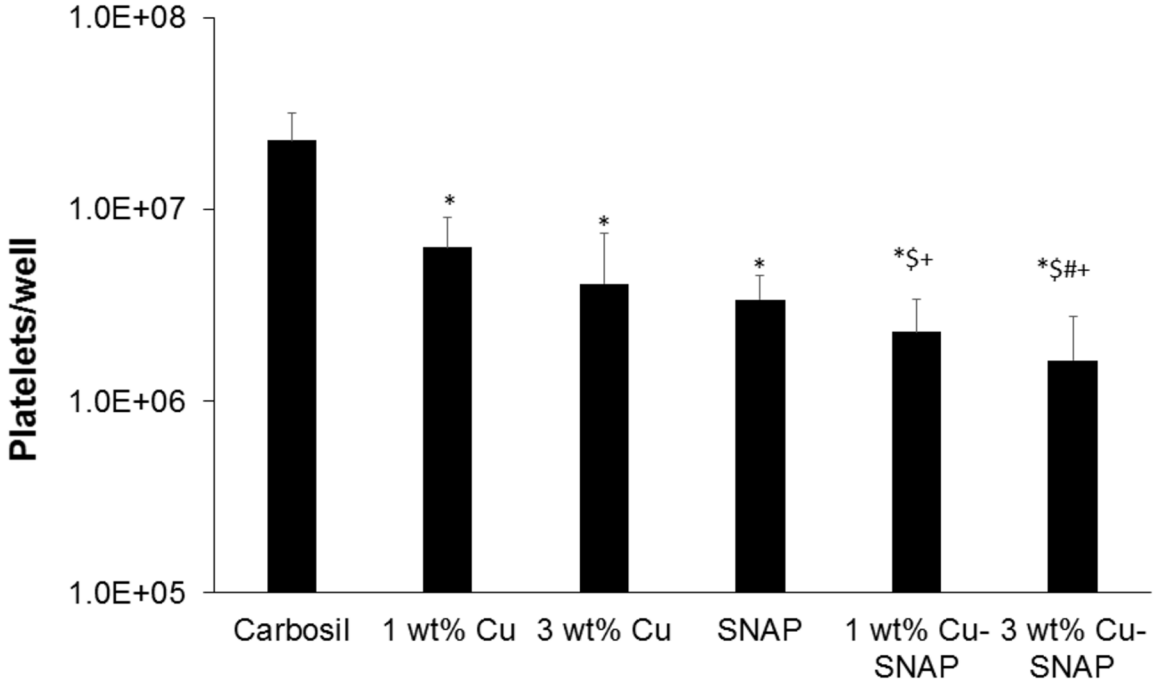

Figure 5.

The graphical representation of the LDH assay results demonstrating the ability of Cu-NPs incorporated SNAP films to reduce platelet adhesion after exposure to porcine platelet rich plasma (PRP) in a 2 h study. The 3 wt% Cu-SNAP provided the largest decrease in platelet adhesion, showing a 92% reduction when compared to controls ($p = 0.003$). P-values < 0.05 were considered significantly different. Note: * indicates significant difference with respect to (w.r.t) the control; $ indicates significant difference w.r.t 1 wt% Cu-Carbosil films; # indicates significant difference w.r.t the 3 wt% Cu-Carbosil films and + indicates significant difference w.r.t the SNAP films. The error bar represents standard deviation.

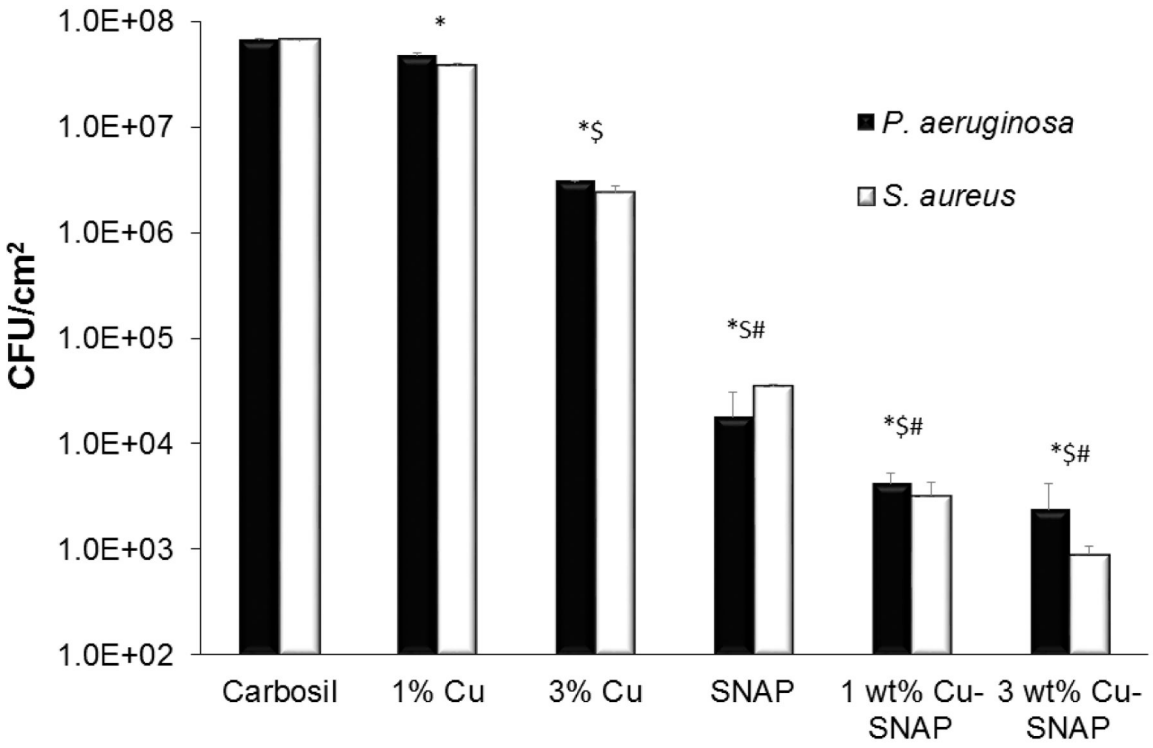

Figure 6.

Graphical representation of inhibition of viable gram-negative (*P. aeruginosa*) and gram-positive (*S. aureus*) bacteria strains on the surface of control and test composites. The 3 wt% Cu-SNAP films showed lowest amount of CFU/cm^2 on the composite surface as compared to any other composites tested (with or without Cu-SNAP) owing to the highest NO flux it released. P-values < 0.05 were considered significantly different. Note: *, $, and # indicate significant difference in CFU/cm^2 of both bacteria compared to control, 1 wt% Cu, and 3 wt % Cu-Carbosil composites, respectively. The error bar represents standard deviation.

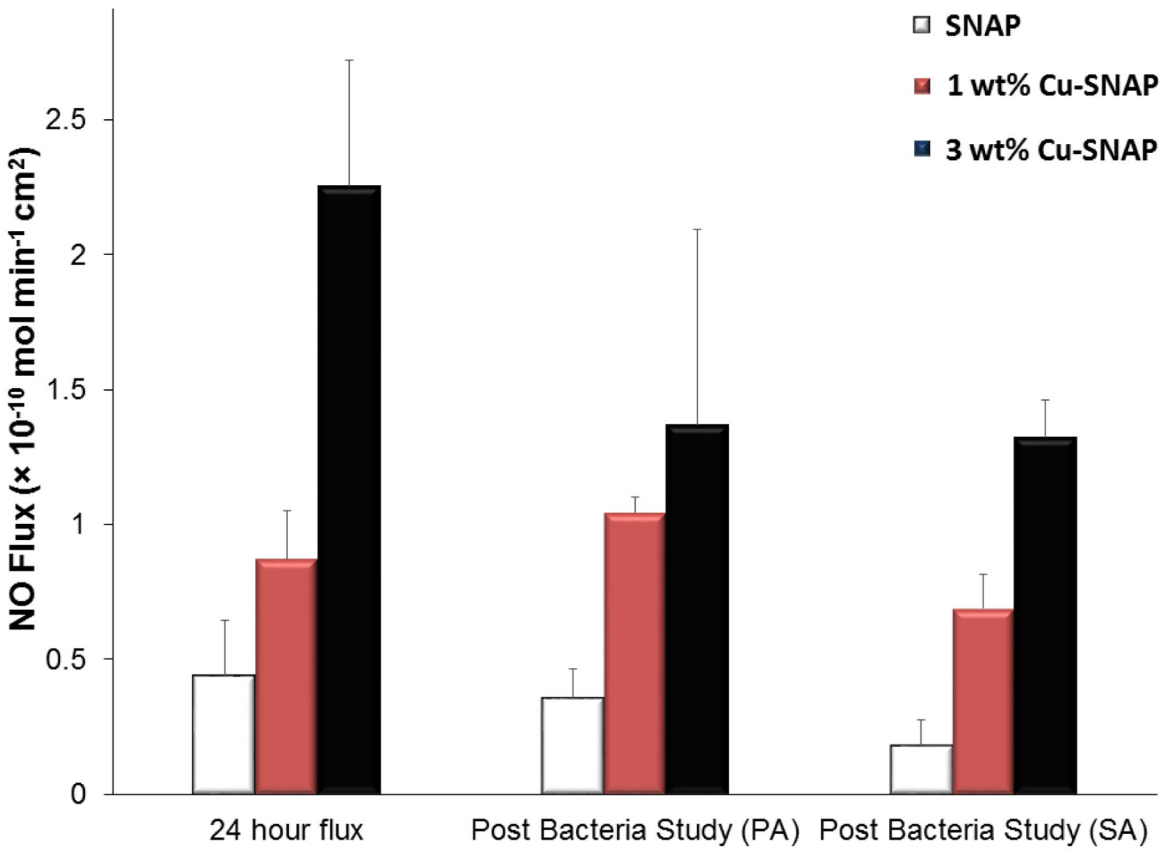

Figure 7.

The NO flux release from the SNAP, 1 wt% Cu-SNAP and 3 wt% Cu-SNAP films at 24th hour prior to exposing them to the bacteria (left most bars). Post bacterial exposure individually with *Pseudomonas aeruginosa* (PA) and *Staphylococcus aureus* (SA) for a period of 24 h, the NO flux released was measured again and found to be in the physiological range. P-values < 0.05 were used for comparison. The error bar represents standard deviation.

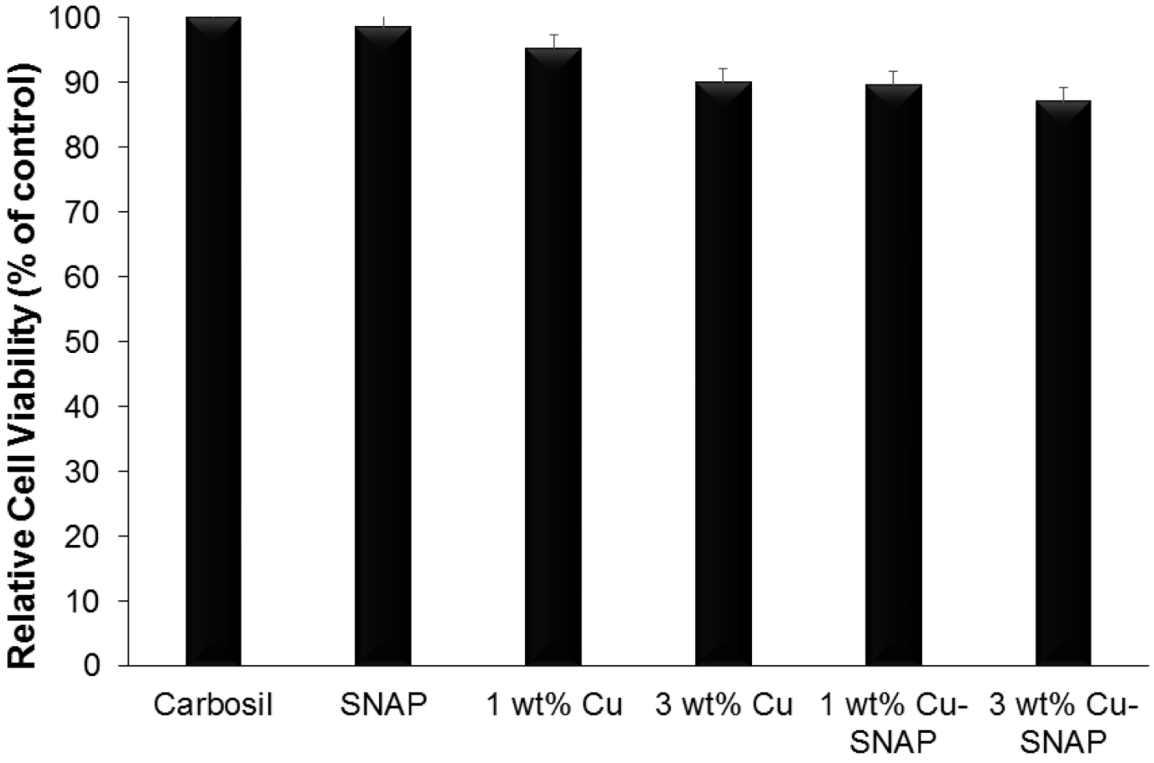

Figure 8.

Graph showing the non-cytotoxic nature of the films using CCK-8 assay performed *in vitro* on mouse fibroblast 3T3 cell line with 24 h leachable from the composites. P-values < 0.05 were used for comparison. The error bar represents standard deviation.

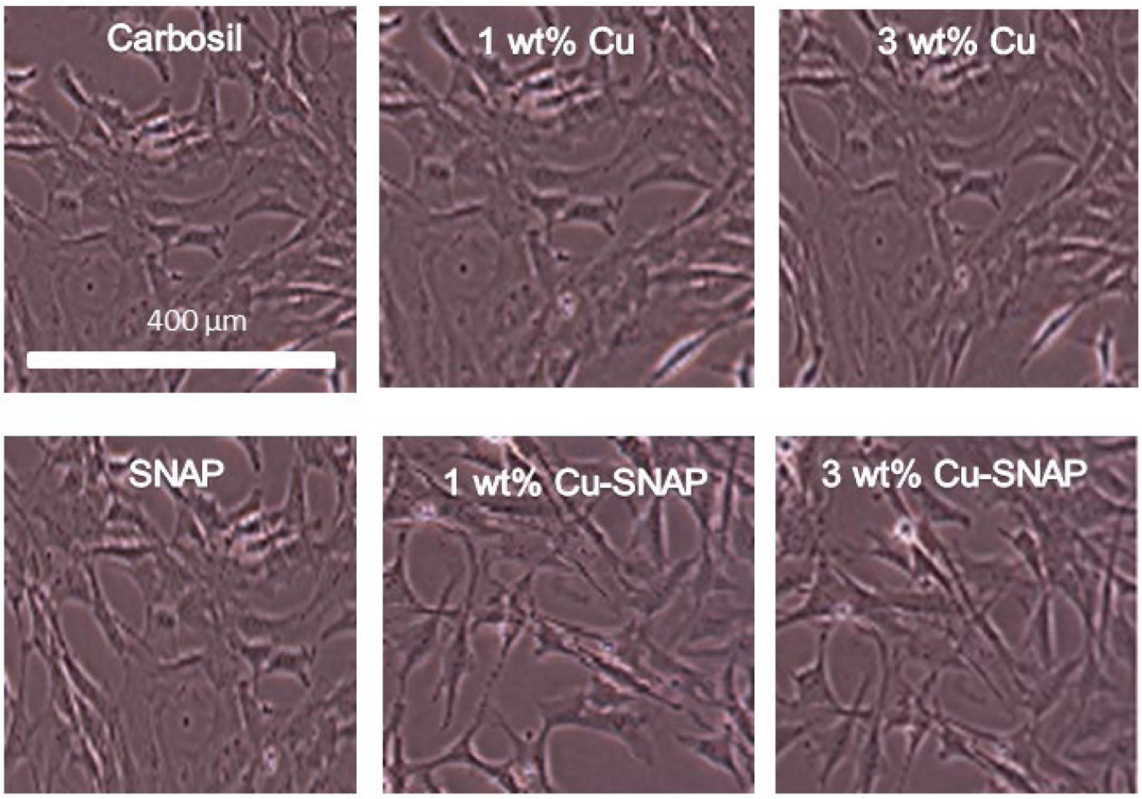

Figure 9.

Representative optical images of 3T3 fibroblast cells after 24 h leachates treatment taken at 10X magnification using EVOS XL microscope. No observable difference in the morphologies of the fibroblast cells was found with respect to the control.

Table 1.

The copper leachate concentration from polymeric composite and the relative leaching in DMEM medium as compared to the original amount of copper present in each film type.

Sample	Measured Copper Leachate (PPB)	% Copper Leaching (Relative to Initial Cu concentration)
1 wt% Cu-NPs	100.3±17.48	1.06±0.185
1 wt% Cu-SNAP	221.5±47.80	2.34±0.506
3 wt% Cu-NPs	93.37±5.995	0.329±0.0212
3 wt% Cu-SNAP	306.9±99.50	1.08±0.351

Table 2.

The comparative analysis of bacterial CFU/cm^2 grown on with Carbosil, Cu-NPs, SNAP, and Cu-SNAP composites.

	NO Flux (× 10^{-10} mol^{-2}min^{-1}cm^{-2})			
Films	**0h**	**24h post bacteria**	**CFU/cm^2 (*S. aureus*)**	**CFU/cm^2 (*P. aeruginosa*)**
Control (Carbosil)	--	--	6.7± 0.1 × 10^7	6.8 ± 0.1 × 10^7
1 wt% Cu	--	--	3.8 ± 0.22 × 10^7	4.8 ± 0.22 × 10^7
3 wt% Cu	--	--	2.4 ± 0.33 × 10^6	3.1 ± 0.33 × 10^6
SNAP	1.31 ± 0.6	0.43 ± 0.1	3.5 ±1.3 × 10^4	1.8 ± 1.3 × 10^4
1 wt% Cu-SNAP	4.48 ± 0.5	0.87± 0.1	3.2 ±1.1 × 10^3	4.2 ± 1.1 × 10^3
3 wt% Cu-SNAP	4.84 ± 0.2	2.25 ± 0.3	8.9 ±1.8 × 10^2	2.4 ± 1.8 × 10^2